

Coupling machine learning with 3D bioprinting to fast track optimisation of extrusion printing[☆]

Kalani Ruberu^{a,#}, Manisha Senadeera^{b,#}, Santu Rana^b, Sunil Gupta^b, Johnson Chung^a, Zhilian Yue^a, Svetha Venkatesh^{b,*}, Gordon Wallace^{a,*}

^a Intelligent Polymer Research Institute, ARC Centre of Excellence for Electromaterials Science, AIIIM Facility, Innovation Campus, University of Wollongong, NSW, Australia

^b Applied Artificial Intelligence Institute (A2I2), Deakin University, Geelong, VIC, Australia

ARTICLE INFO

Article history:

Received 14 October 2020

Revised 25 November 2020

Accepted 5 December 2020

Keywords:

3D Bioprinting

Machine learning

Bayesian optimisation

Gelatin methacryloyl

Hyaluronic acid methacrylate

ABSTRACT

3D bioprinting, a paradigm shift in tissue engineering holds a promising perspective for regenerative medicine and disease modelling. 3D scaffolds are fabricated for subsequent cell seeding or incorporated directly to the bioink to create cell-laden 3D constructs. A plethora of factors relating to bioink properties, printing parameters and post print curing play a significant role in the optimisation of the printing process. Although qualitative evaluation of printability has been investigated largely, there is a paucity of studies on quantitative approaches to assess printability. Hence, this study explores machine learning as a novel tool to evaluate printability quantitatively and to fast track optimisation of extrusion printing in achieving a reproducible 3D scaffold. Bayesian Optimisation, a machine learning method has been employed for optimising 3D bioplotting with a scoring system established to assess the printability of gelatin methacryloyl (GelMA) and hyaluronic acid methacrylate (HAMA) bioinks. The performance of two fundamental criteria encountered in the printing process: the filament formation of the bioink and the layer stacking of the 3D scaffold have been incorporated in the scoring metric. The optimal print parameters for GelMA containing inks with ranging concentrations (10%, 7.5% & 5% (w/v)) were obtained in 19, 4 & 47 experiments whereas for GelMA:HAMA (10:2%, 7.5:2% & 5:2% (w/v)) 32, 25 & 32 experiments were required respectively. This number of experiments is drastically reduced compared to the 6000 to 10 000 possible combinations in the Bayesian algorithm. Hence, this study will be a stepping-stone into unravelling the benefits of machine learning in this rapidly developing area of 3D bioprinting.

© 2020 Published by Elsevier Ltd.

1. Introduction

3D bioprinting continues to grow exponentially, gaining significant popularity within the fields of regenerative medicine and disease modelling [1]. The term 3D biofabrication has been used in parallel with the term 3D bioprinting and can be defined as a computer-guided additive manufacturing technique for creating highly precise and complex 3D structures with biologically relevant materials in a pre-designed geometry [2,3]. The cells of interest are either seeded on to the printed constructs or alternatively incor-

porated directly to the bioink prior to creating cell-laden 3D patterned constructs [4]. Subsequently, these bioscaffolds are provided with the essentials of a cellular microenvironment to achieve adequate cell proliferation and/or differentiation in a 3D platform simulating the real-life scenario. Since such approaches offer an enormous potential to recreate multi-faceted organisation of tissues, researchers are actively studying this 'biofabrication space', not to mention, the substantial advancements in the cartilage, bone, liver, skin & vascular tissue fabrication to date [5–9].

Bioinks are a fundamental part of the bioprinting process and act as the delivery medium for cells and growth factors, and more importantly the supportive materials for cells to adhere, proliferate and thrive post printing [10]. While maintaining cytocompatibility, an ideal bioink should accommodate two key physical characteristics, 'printability' to form a successful 3D construct and 'high mechanical stability' to enable good shape fidelity of the printed structure [11]. Hence, a bioink that transmits through the 3D printer should preferably adopt a fluidic nature with reasonable

[☆] This work was conducted using a Bayesian Optimization software developed by A2I2. If you would like to use the software please contact: manisha.senadeera@deakin.edu.au

* Corresponding authors.

E-mail addresses: svetha.venkatesh@deakin.edu.au (S. Venkatesh),

gwallace@uow.edu.au (G. Wallace).

Equally contributed to this study.

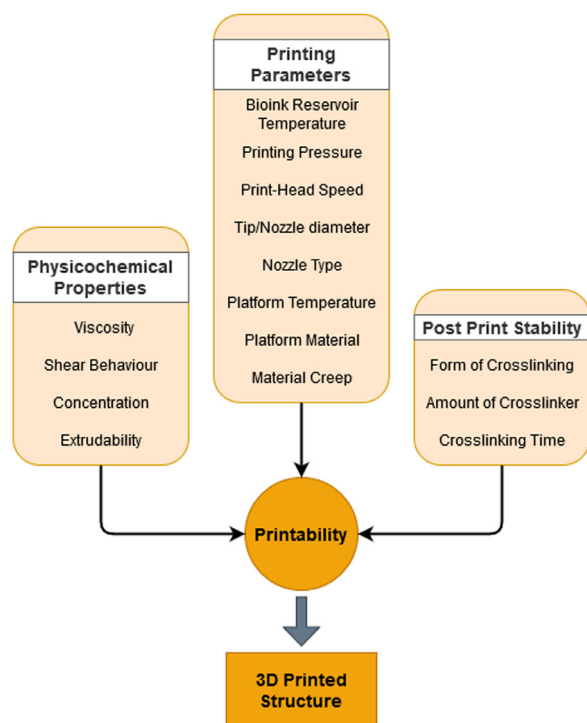


Fig. 1. Overview of the parameters contributing towards printability of bioinks: Physicochemical properties of the bioink, Printing parameters and Post print stability play an important role in achieving a good 3D printed structure.

printability during its extrusion process, and subsequently undergo a phase transition to maintain sufficient structural integrity of the 3D print over long incubation periods in cell culture [2]. On par with previous research, it is noted that a plethora of factors relating to physicochemical properties, printing parameters and post print curing play a significant role in printability optimisation of any bioink (Fig. 1). Rheology of a bioink is predominantly dependant on its viscoelastic and shear behaviour [12], which in turn rely greatly on the concentration of the ink formulation [13]. Furthermore, the extrudability and extrusion uniformity of the bioink [14] have also been reported as contributing towards printability. Apart from physical characteristics of the bioink, modifiable functions of the 3D printer play a huge role in accomplishing a good print. Ink reservoir temperature, printing pressure, nozzle diameter, nozzle type, print-head speed and temperature of the platform can easily be adjusted accordingly to increase printability [15,16]. Finally, the structural integrity to form a self-supporting 3D scaffold is realised by stimulating gelation of the bioink, which is achieved by employing a suitable method of crosslinking. Photo [17,13], chemical [18] and thermal [19] crosslinking are carefully chosen depending on the chemistry of the bioink formulation. The amount of crosslinker used [20] and the time of crosslinking [10] determine the degree of rigidity of the self-assembled 3D construct.

Fine-tuning such a myriad of variables to accomplish a reproducibly printable 3D scaffold can be a tedious and a time-consuming process. Failure to do so however could result in either a continuously clogging nozzle or a collapsing 3D print with poor mechanical integrity. Despite the number of previous investigations on printability optimisation, such as, rheological characteristics of bioinks [21,22,23], mathematical modelling on bioink flow behaviour [24,11,23] and image analysis of the printed scaffolds [11], researchers still rely largely on trial and error experimentation for fabricating 3D scaffolds with good shape fidelity.

As such there is a growing need for an alternate and rapid method for printability evaluation and optimisation of bioinks. Machine Learning is a proven and effective method in this regard and can enable full automation of the process and decrease experimentation time. Compared to classical Design of Experiment (DoE) methods which determine a sampling pattern prior to taking observations, machine learning methods can employ adaptive sampling during the experimentation process. This approach also enables development of a database to predict printability and to make recommendations to the experimenter. The benefits of applying machine learning to 3D bioprinting is only recently being realised with studies conducted into printing prediction [25] and optimisation [26] using inkjet based bioprinting. Many of these approaches however have required large amounts of data to construct the machine learning model.

In contrast, modern machine learning methods can model a black-box function with a minimal amount of experimental data [27]. This method is increasingly being applied for the efficient design of novel materials and processes [28,29]. This becomes important when experimentation is expensive as in our case. This study implemented a method of machine learning known as Bayesian optimisation (BO) to achieve the goal of finding the optimal parameters with minimum experimentation. BO is a well-known sample-efficient method to adaptively find the global optima of a black-box function and has theoretical guarantees of convergence [30]. BO provides advantages over other optimisation methods such as genetic algorithms and derivative-free local optimisers, which require a large number of samples, and gradient-based methods, where gradient information is required. Due to the large number of possible factors that can be adjusted, this system is ideal to accommodate the numerous variables that need to be altered during the printing process, hence BO provides an efficient means of searching the printer setting space to find settings that will produce an optimal print.

Herein we present for the first-time coupling Bayesian optimisation, a collaborative and flexible algorithm with 3D bioprinting to accelerate printability optimisation of bioinks for extrusion printing. A range of concentrations of gelatin methacryloyl (GelMA), and GelMA/hyaluronic acid methacrylate (HAMA) were selected as examples for optimisation.

2. Experimental section

2.1. Preparation of GelMA and GelMA/HAMA bioinks

2.1.1. Preparation of GelMA

GelMA blended from ~300 bloom gelatin type A (synthesized as described previously in [31]) was used to prepare 5%, 7.5% & 10% (w/v) concentrated solutions. Appropriate amounts of freeze-dried GelMA flakes were dissolved in cell culture grade phosphate buffered saline (Sigma) containing 100 U mL⁻¹ penicillin and streptomycin 100 µg mL⁻¹ (Gibco) in a laminar flow. The bioinks were heated at 37 °C with intermittent vortexing to accelerate dissolution.

2.1.2. Preparation of GelMA/HAMA

GelMA solutions (5%, 7.5% and 10% (w/v)) were prepared respectively as described previously in Section 2.1.1, followed by the addition of 2% (w/v) HAMA (synthesized as described in [31]). GelMA/HAMA composite bioinks were heated at 37 °C while vortexing vigorously until formation of a homogeneous viscous gel.

2.2. Addition of photo-initiator to the bioinks

Irgacure 2959 (Sigma) was used as the chosen photo-initiator for GelMA and GelMA/HAMA bioinks. 10% (w/v) Irgacure 2959 was

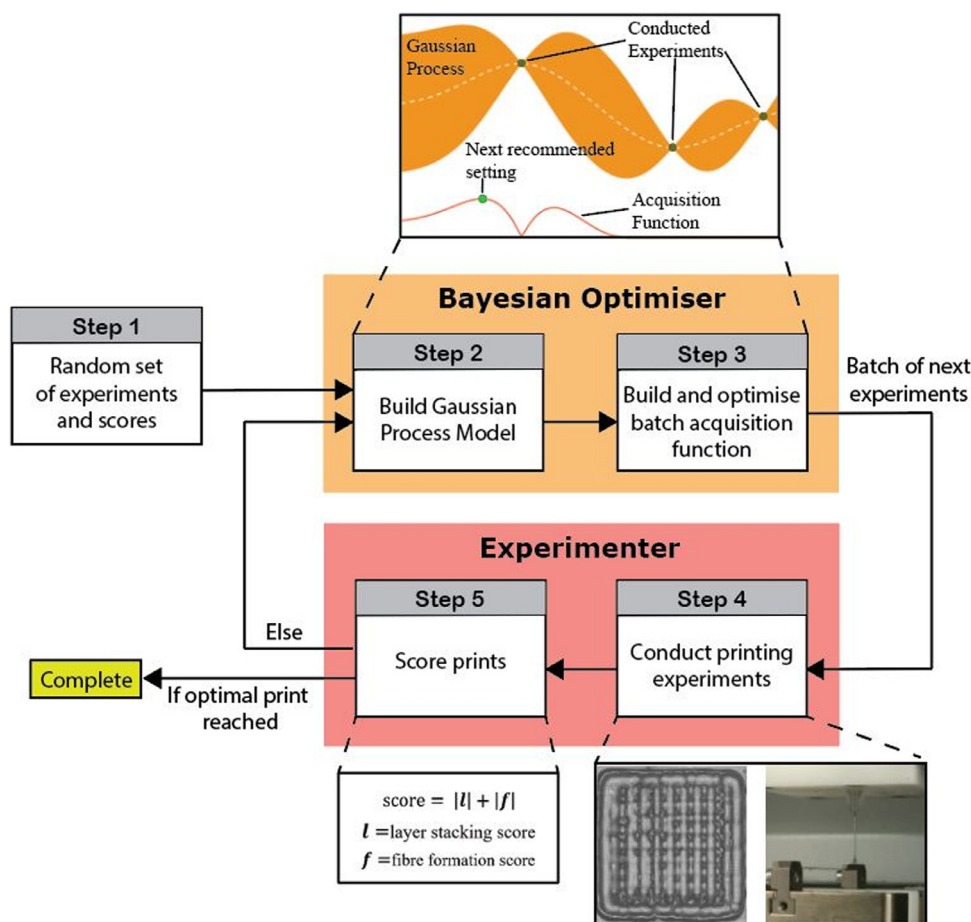


Fig. 2. Bayesian Optimisation framework.

prepared in 100% ethanol and added to GelMA and GelMA/HAMA bioinks respectively, to a final concentration of 0.2% (w/v).

The photo-initiator containing bioink/blends were transferred to 30CC printer reservoir (Nordson EFD) using 1 mL disposable syringes (Terumo). The printer reservoir was centrifuged (Heraeus Primo R, Thermofisher) at 1500 rpm for 5mins to remove any trapped air bubbles from the bioink. Subsequently the bioink loaded printer reservoirs were covered in aluminium foil to protect from exposure to light and stored in the refrigerator for at least 15 hrs prior to printing.

2.3. Printing of GelMA and GelMA/HAMA bioinks

Extrusion printing was carried out using the EnvisionTEC 3D Bioplotter (GmbH Germany). The inks involved in the study include 10%(w/v) GelMA, 7.5% (w/v) GelMA and 5% (w/v) GelMA, 10:2% (w/v) GelMA/HAMA, 7.5:2% (w/v) GelMA/HAMA and 5:2% (w/v) GelMA/HAMA, providing a wide range of viscosities that span from low, medium to high. Lattice structures ($10 \times 10 \times 2.5$ mm) with 500 μ m strand width and 130 μ m splicing were fabricated. Constructs were printed using 27-gauge precision stainless steel nozzle (200 μ m Nordson EFD). Following deposition of each layer, 20 s of UV exposure with an intensity of 530 mW/cm² (365 nm, Omnicure S1000) was applied to initiate crosslinking of the printed ink and hence stabilise each layer. A range of parameters were investigated, including bioink reservoir temperatures, pressures, print-head speeds and platform temperatures as according to the output variable values predicted by the 'black-box system' (described in Section 2.5).

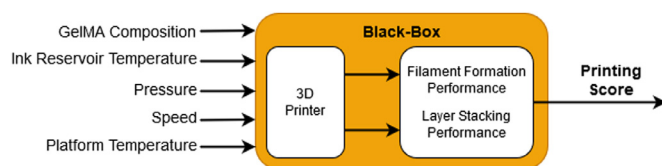


Fig. 3. System to be optimized.

2.4. Imaging of filament formation & layer stacking of GelMA and GelMA/HAMA bioinks

Extruding filaments at a tear-off speed of 2 s from different experimental sets predicted from Bayesian Optimisation were imaged from a constant distance with the use of an iphone. The layer stacking and the pore architecture were captured by the in-built camera in the EnvisionTEC 3D Bioplotter.

2.5. Bayesian optimization framework

Fig. 2 illustrates the framework applied for bioprinting optimisation. The framework began with a set of randomly conducted and scored experiments. These experimental results, made of pairs of printer settings and their associate printing score, were used to initialise the Bayesian optimiser. Within the optimiser, a probabilistic model of the system (as defined in Fig. 3) is built and used to recommend the next batch of experiments (printer settings) to be conducted.

Table 1
Parameter limits at beginning of experimentation.

	GelMA	GelMA/2% HAMA	Step Size
GelMA Composition (%)	5, 7.5, 10	5, 7.5, 10	–
Ink Reservoir Temperature (°C)	20 – 25	24–29	1
Pressure (bar)	2–3	2.5–3.5	0.1
Speed (mm/s)	10–20	8–18	0.5
Platform Temperature (°C)	10	10	1

The experiments were communicated back to the experimenter who then conducted printer tests with the recommended settings and scored the performance. These results were then fed back into the optimiser and the loop continued until an optimal print was reached. Further details of the framework components are discussed below.

2.5.1. The Bayesian Optimiser

The framework begins with the Bayesian Optimiser being provided a randomly conducted set of variable bioink compositions and printer settings and their associated printing score based on the performance of filament formation and layer stacking. Input variables for the bioink compositions consisted of three GelMA concentrations and three GelMA/HAMA concentrations whereas the input variables for the printer settings comprised of bioink reservoir temperature, extrusion pressure, print-head speed and the platform temperature. Fig. 3 illustrates the system being optimised. The system contains many complex relationships between the input variables and the output printing score and as such we consider it to be a black-box system. To overcome this and achieve our search goal, the Bayesian optimiser uses past experimental data to build a probabilistic estimate of the black-box system modelled through a Gaussian process. A Gaussian process is fully defined by a mean function and a covariance function [32]. The covariance function, calculated using the squared exponential kernel [32] in this case, expresses smoothness over the function i.e. how the printing score value at one location influences the estimate of the values around it. The mean and covariance from the model were used to construct an acquisition function which is optimised to recommend the next printer settings to test. This recommended printer setting is defined to be where the Bayesian Optimiser expects the chance of finding an optimal printing score is the highest. Exploration and exploitation were balanced via the acquisition function to ensure the space of settings was searched efficiently to find the optima. The Expected Improvement acquisition function was applied [33].

For this project, experimental recommendations provided by the optimiser were given in a batch to the experimenter in each iteration, to allow the experimenter to conduct and score multiple experiments in one go. Some inputs were constrained in that their values were required to be constant across an experimental batch to allow for ease of experimentation. 3 – 10 experimental recommendations per iteration were deployed and the constrained printer parameters were the temperature of the bioink reservoir and the platform. This method is known as process-constrained batch Bayesian Optimisation and operates by first optimising for the constrained parameters, and then holding them constant across the remaining recommendations in the experimental batch [34].

2.5.2. The search space

Table 1 details the ranges for each of the printer parameters at the start of experimentation including the discretised step size.

Printer settings for each of the six GelMA compositions were sought after, and as such six streams of experimentation were conducted.

Table 2
Updated parameter discretisation's determined through collaboration between the Bayesian Optimisation algorithm and the experimenter.

	GelMA	GelMA/2% HAMA	Step Size
GelMA Composition (%)	5, 7.5, 10	5, 7.5, 10	–
Ink Reservoir Temperature (°C)	1	1	1
Pressure (bar)	0.1	0.1	0.1
Speed (mm/s)	0.1	0.1	0.1
Platform Temperature (°C)	1	1	1

2.5.3. Print scoring

A scoring system was introduced for both filament morphology during extrusion and the pore architecture on layer stacking to assess these proxy measurements of printability quantitatively. Fig. 4 and pages 1–2 in supplementary data illustrate the scale used by the experimenter to assess the performance of a print. In the case of printing filament, a negative score indicates under-gelation and droplet formation, while a positive (non-zero) value indicates over-gelation and no fibre formation. A similar system applies to the pore architecture on layer stacking, where an ideal score for each feature is '0'.

For the Bayesian optimisation search, a single value acts as the output for the 'black-box function'. As there are two print features to optimise: the printing filament morphology and the pore architecture on layer stacking, the performance on these two metrics are combined.

The print score inputted into the Bayesian Optimiser was calculated as the sum of the absolute value of the Layer stacking score and the Filament morphology score as shown in Eq. (1). The objective of BO was to optimise print performance, in this case minimise the print score. If the print score output is '0', an ideal print setting was found and experimentation ceases.

$$\text{Print score} = |\text{Layer Stacking Score}| + |\text{Filament Morphology Score}| \quad (1)$$

3 Results & discussion

Search space expansion & validation

The experiments conducted in the first iteration were randomly selected to initialise the Gaussian Process model in the BO algorithm. After experimentation began, it was observed that changes were needed to be made to the ranges of the printer parameters. Initially the ranges were limited to that shown in Table 1, but as experimentation continued, it became clear that expansion of the ranges and finer discretisation of the step size was needed to reach the optima. These included changing the batch size, from 10 experiments in early iterations, down to 3 in later iterations due to resource availability. The ranges of the input parameters were also adjusted during the experimentation process. These adjustments were made when the experimenter observed the algorithm conducting extensive searching at the limits of a given input parameter. The final discretisation's are shown in Table 2 and the changes in the printing parameter ranges including the experimental results are presented in Fig. 5& Fig. 6. This indicated there was potential for better printing scores to be achieved beyond the current ranges, and as such the ranges were extended appropriately. At other times, the step size was reduced to allow for finer resolution experimentation. All these changes were made upon the observations made by the human experimenter, and when implemented in the algorithm, had no disruption to the operations and performance of the BO algorithm, including not wasting any previously conducted experiments. The ability to make such adjustments during the experimentation process illustrates the collaboration process between the algorithm and the experimenter, whereby the ex-

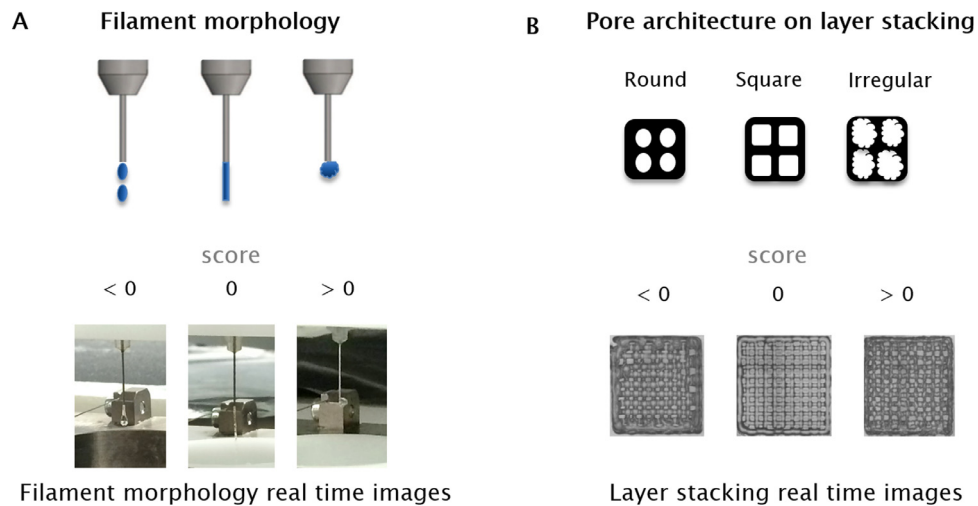


Fig. 4. Evaluation of bioink printability by two fundamental criteria: printing filament morphology during extrusion from needle tip and pore architecture on layer stacking. A) Schematic representation and real time images of filament morphology. B) Schematic representation and real time images of pore architecture on layer stacking of 10×10 mm lattice structures.

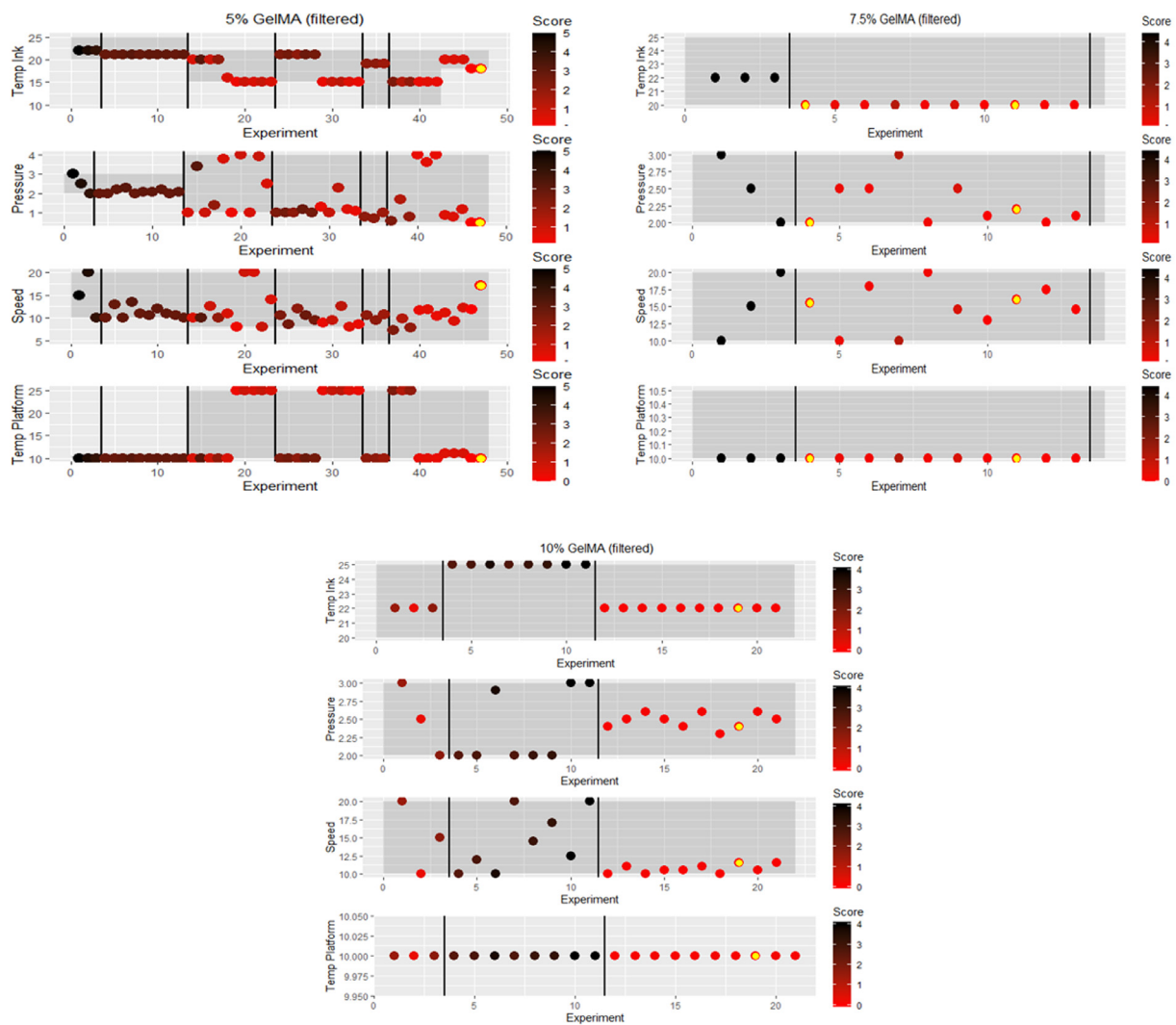


Fig. 5. Results of 5%, 7.5% & 10% (w/v) GelMA experiments. Black vertical lines segment between batches. Circles indicate score for a given experiment (red = better print). Shaded region is range for a given printing parameter. Yellow dot indicates optimal print.

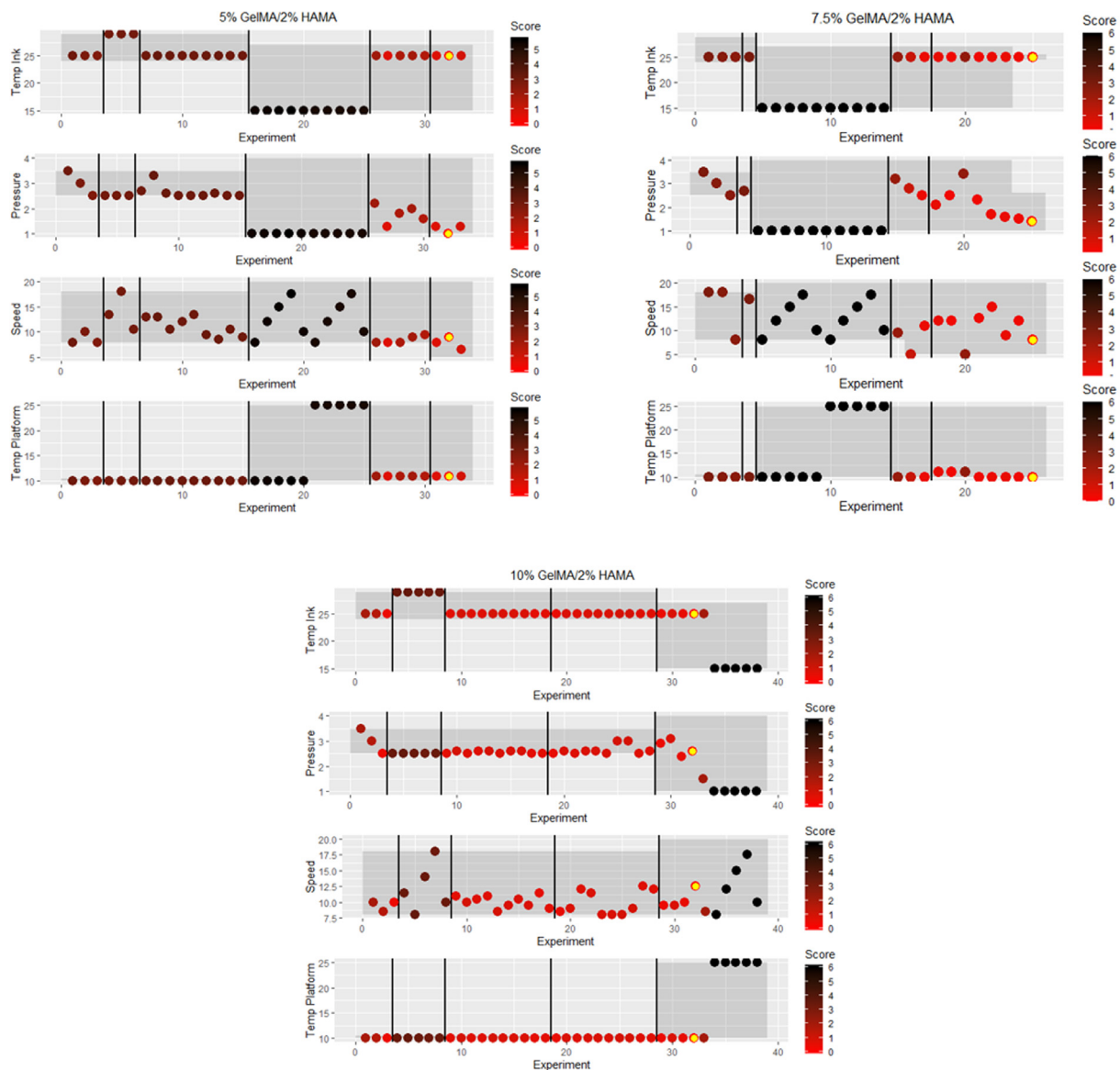


Fig. 6. Results of 5%, 7.5% & 10% (w/v) GelMA: 2% (w/v) HAMA experiments. Black vertical lines segment between batches. Circles indicate score for a given experiment (red = better print). Shaded region is range for a given printing parameter. Yellow dot indicates optimal print.

perimeter is able to observe the behaviour of the algorithm and the results of the search, and make changes appropriately without impacting the process.

Printability evaluation

BO is employed for the printability refinement on extrusion printing, the most widely explored form of 3D bioprinting technique [11]. GelMA and HAMA bioinks were chosen as good candidates for our project as these versatile bioinks not only hold the ability to mimic the native extracellular matrix of a multitude of tissues [10,35,31] but also possess high viscosity which is a crucial physical characteristic that is best suited for extrusion printing [36]. Printability of GelMA and GelMA/HAMA bioinks was assessed quantitatively by two criteria namely the filament morphology during the extrusion process and the pore architecture on layer stacking [11,23].

Consistent with previous research [11], the bioink status at the needle tip would exhibit three clear variations, which include formation of i) droplets, ii) a continuous filament or iii) an irregular shape due to over-gelation as shown in Fig. 4A. Demonstration of a

homogeneous thin filament which hangs from the tip of the nozzle is scored a '0', hence considered a good measure of printability for GelMA and GelMA/HAMA blends [13]. Bioink reservoir temperatures of 22 °C, 20 °C & 18 °C revealed ideal filament formation for 10%, 7.5% & 5% (w/v) GelMA respectively (Table 4, Fig. 5, Table 1 in supplementary data) whereas a slightly elevated reservoir temperature of 25 °C scored '0' for the filament morphology of all three concentrations of GelMA/HAMA (Table 4, Fig. 6, Table 2 in supplementary data).

Moreover, the ability of fabricating a defined 3D construct, in this case a lattice with clear pore architecture was highly correlated to the nature of the extruded filament [11]. Droplet formation during extrusion will result in a 3D construct with small round pores while an over-gelated bioink would produce a construct with irregular shaped pores as clearly shown in Fig. 4B. Hence, a bioink at its proper-gelation status will form a standard lattice containing distinct square pores with improved shape fidelity, scoring a '0'.

A print score is achieved for each experiment performed, by tallying the two values of the filament formation score and the layer stacking score and returning a single print score as defined

Table 3

Print scoring for Bayesian Optimisation Search: Some examples of GelMA showing the printability measurement as the combination score of filament morphology and layer stacking performance using Equation 1.

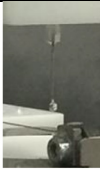
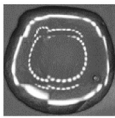



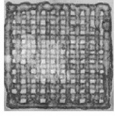
	Filament Morphology Score	Layer Stacking Score	Print Score
5% (w/v) GelMA @ 22°C and 2.5bar pressure	 -1.9	 -3	4.9
7.5% (w/v) GelMA @ 22°C and 2.5bar pressure	 -1.5	 -2.5	4.0
10% (w/v) GelMA @ 22°C and 2.5bar pressure	 0	 -0.1	0.1

Table 4

Optimised 3D Printing Parameters for EnvisionTEC Bioplotter through Bayesian Optimisation algorithm.

Parameter	Printer settings for GelMA		
GelMA Composition% (w/v)	5	7.5	10
Ink Reservoir Temperature (°C)	18	20	22
Pressure (bar)	0.5	2	2.4
Speed (mm/s)	17.2	15.5	11.5
Platform Temperature (°C)	10	10	10

Parameter	Printer settings for GelMA/HAMA		
GelMA/HAMA Composition% (w/v)	5:2	7.5:2	10:2
Ink Reservoir Temperature (°C)	25	25	25
Pressure (bar)	1	1.4	2.6
Speed (mm/s)	9	8	12.5
Platform Temperature (°C)	11	10	10

in Eq. (1). Some examples of varied concentrations of GelMA prints are shown in Table 3. An overall print score of '0' demonstrates the optimal printing conditions for GelMA and GelMA/HAMA blends (yellow dots in Figs. 5& 6) where a reproducible 3D print is executed from extrusion printing using the EnvisionTEC bioplotter. Table 4 and Figs. 5& 6 display the experimental results, with the shaded region indicating the range for each of the printing parameters, and the black line segmenting each batch. Out of a space of between 6000 and 10,000 possible printing settings, the Bayesian Optimisation algorithm was able to discover the optimal printer setting in as few as 19, 4 & 47 experiments for 10%, 7.5% & 5% (w/v) GelMA respectively and 32, 25 & 32 experiments 10%, 7.5% & 5% (w/v) GelMA: 2% (w/v) HAMA in experiments respectively.

Hence, Bayesian Optimisation was able to accelerate the experimentation process, conducting the search for optimal parameters according to conditions specified by the experimenter. Additionally, the algorithm was able to adapt based on insights provided by the researcher during the experimentation process, leading to fast convergence towards optimisation.

Reflection of experimental process

In the experiment, the scoring of a print was manually conducted via a visual assessment by the experimenter. The process involved taking photos, like those shown in Table 3, and comparing the images against the scale (shown in Fig. 4) to decide upon a score. As this is done by sight, much of the scoring is prone to human errors of judgements, and as such may not reflect a consistent objective measure of the print performance. Though the Gaussian Process model can handle errors in measurement (referred to as noise), this can impact the performance of the optimiser and result in more experiments being needed to find the optima. An additional factor contributing to an extension of the number of experiments needed to reach the optima is the experimental batch size. When a batch is recommended by the Bayesian optimiser, the confidence of achieving a good print is ranked down from the first recommendation of a batch (strongest confidence), with the least confident recommendation proposed at the end of the batch. In our experiments we initially started with a batch size of 10. With a large batch size, there is a chance that some experiments in the batch were recommended with far less confidence but were still provided in order to meet the batch size. As such smaller batch sizes were recommended in later iterations. Ideally, a batch size of 1 would lead to the lowest number of experiments being needed but will require the experimenter to undertake more visits to the lab and set up the printer to perform a single experiment on each occasion.

4. Conclusion

This study investigated the prospects of coupling machine learning to optimise printability of extrusion printing of GelMA and GelMA/HAMA bioinks in the EnvisionTEC 3D Bioplotter to achieve a reproducible 3D print with good shape fidelity. Bayesian optimisation, a sample efficient optimisation algorithm was applied in our experimental process with the goal to attain the optimal printing parameters with minimal number of experiments.

Six varied bioink concentrations (10%, 7.5% & 5% (w/v) GelMA and 10:2%, 7.5:2% & 5:2% (w/v) GelMA:HAMA) and a number of printer settings (bioink reservoir temperature, extrusion pressure, print speed and the platform temperature) were inputted into the Optimiser Search Space, and the output recommendations predicted by the 'black-box' model were provided to the experimenter. A scoring system was established via a visual assessment on filament morphology during extrusion from the needle tip and the pore architecture on layer stacking of the 3D scaffold, where the experiment ceased when an optimal total score of '0' was achieved. The BO method employed here is a concerted approach where the experimenter is guided by the algorithm nevertheless it has the self-tuning capability to adapt based on the insights provided by the experimenter with zero disruptions to its performance.

Our results demonstrate a novel, quantitative approach to extrusion printability optimisation of GelMA and GelMA/HAMA bioinks. This Bayesian optimisation technique can be readily applied to printability optimisation of other types of (bio)ink systems where extrusion-based modality is employed. Furthermore, it is evident that BO was able to successfully accelerate the extrusion bioprinting experimentation process in comparison to the traditional trial and error optimisation that can be tedious and also time-consuming. We believe, this study will be a seminal body of work unravelling the benefits of machine learning in various aspects of this fast-developing 3D bioprinting arena.

Author Contributions

Kalani Ruberu: Conceptualization, Methodology, Validation, Formal analysis, Investigation, Data Curation, Writing – Original Draft, Writing – Review & Editing, Visualisation

Manisha Senadeera: Conceptualization, Methodology, Software, Formal analysis, Investigation, Data Curation, Writing – Original Draft, Writing – Review & Editing, Visualisation

Santu Rana: Conceptualization, Methodology, Writing – Review & Editing, Supervision

Sunil Gupta: Conceptualization, Supervision

Johnson Chung: Methodology, Writing – Review & Editing

Zhilian Yue: Conceptualization, Methodology, Writing – Review & Editing

Svetha Venkatesh: Conceptualization, Resources, Writing – Review & Editing, Funding Acquisition

Gordon Wallace: Conceptualization, Resources, Writing – Review & Editing, Funding Acquisition

Declaration of Competing Interest

The authors declare that they have no known competing financial interests or personal relationships that could have appeared to influence the work reported in this paper.

Acknowledgments

The authors acknowledge funding from the [Australian Research Council](#) (ARC) (CE140100012) and (FL170100006), and support from the [Australian National Fabrication Facility](#) (ANFF) – Materials Node & the Translational Research Initiative for Cellular Engineering and Printing (TRICEP).

Supplementary materials

Supplementary material associated with this article can be found, in the online version, at [doi:10.1016/j.apmt.2020.100914](https://doi.org/10.1016/j.apmt.2020.100914).

Appendix

Scoring Experimental data with images and Overall Score Table can be found in the Supplementary Information.

References

- [1] V. Mironov, T. Boland, T. Trusk, G. Forgacs, R.R. Markwald, Organ printing: computer-aided jet-based 3D tissue engineering, *Trends Biotechnol.* 21 (2003) 157–161.
- [2] V. Mironov, N. Reis, B. Derby, Review: bioprinting: a beginning, *Tissue Eng.* 12 (2006) 631–634.
- [3] B. Starly, R. Shirwaiker, in: *3D Bioprinting Techniques, 3D Bioprinting and Nanotechnology in Tissue Engineering and Regenerative Medicine*, Academic Press, 2015, pp. 57–77.
- [4] R. Landers, U. Hubner, R. Schmelzeisen, R. Mulhaupt, Rapid prototyping of scaffolds derived from thermoreversible hydrogels and tailored for applications in tissue engineering, *Biomaterials* 23 (2002) 4437–4447.
- [5] B.A.G. Melo, Y.A. Jodat, S. Mehrotra, M.A. Calabrese, T. Kamperman, B.B. Mandal, M.H.A. Santana, E. Alsberg, J. Leijten, S.R. Shin, 3D Printed Cartilage-Like Tissue Constructs with Spatially Controlled Mechanical Properties, *Adv. Funct. Mater.* (2019) 29.
- [6] Y. Yan, H. Chen, H. Zhang, C. Guo, K. Yang, K. Chen, R. Cheng, N. Qian, N. Sandler, Y.S. Zhang, H. Shen, J. Qi, W. Cui, L. Deng, Vascularized 3D printed scaffolds for promoting bone regeneration, *Biomaterials* 190–191 (2019) 97–110.
- [7] E.S. Mirdamadi, D. Kalhori, N. Zakeri, N. Azarpira, M. Solati-Hashjin, Liver tissue engineering as an emerging alternative for liver disease treatment, *Tissue Eng. Part B Rev.* (2020).
- [8] L.J. Pourchet, A. Thepot, M. Albouy, E.J. Courtial, A. Boher, L.J. Blum, C.A. Marquette, Human skin 3D bioprinting using scaffold-free approach, *Adv. Healthc. Mater.* 6 (2017).
- [9] S.Y. Hann, H. Cui, T. Esworthy, S. Miao, X. Zhou, S.-j. Lee, J.P. Fisher, L.G. Zhang, Recent advances in 3D printing: vascular network for tissue and organ regeneration, *Transl. Res.* 211 (2019) 46–63.
- [10] M. Hospodiuk, M. Dey, D. Sosnoski, I.T. Ozbolat, The bioink: a comprehensive review on bioprintable materials, *Biotechnol. Adv.* 35 (2017) 217–239.
- [11] L. Ouyang, R. Yao, Y. Zhao, W. Sun, Effect of bioink properties on printability and cell viability for 3D bioplotting of embryonic stem cells, *Biofabrication* 8 (2016) 035020.
- [12] D. Chimene, K.K. Lennox, R.R. Kaunas, A.K. Gaharwar, Advanced bioinks for 3D printing: a materials science perspective, *Ann. Biomed. Eng.* 44 (2016) 2090–2102.
- [13] W. Schuurman, P.A. Levett, M.W. Pot, P.R. van Weeren, W.J. Dhert, D.W. Hutmacher, F.P. Melchels, T.J. Klein, J. Malda, Gelatin-methacrylamide hydrogels as potential biomaterials for fabrication of tissue-engineered cartilage constructs, *Macromol. Biosci.* 13 (2013) 551–561.
- [14] T. Gao, G.J. Gillispie, J.S. Copus, A.K. Pr. Y.J. Seol, A. Atala, J.J. Yoo, S.J. Lee, Optimization of gelatin-alginate composite bioink printability using rheological parameters: a systematic approach, *Biofabrication* 10 (2018) 034106.
- [15] Y. He, F. Yang, H. Zhao, Q. Gao, B. Xia, J. Fu, Research on the printability of hydrogels in 3D bioprinting, *Sci. Rep.* 6 (2016) 29977.
- [16] S. Abdollahi, A. Davis, J.H. Miller, A.W. Feinberg, Expert-guided optimization for 3D printing of soft and liquid materials, *PLoS ONE* 13 (2018) e0194890.
- [17] C. Decker, Light-induced crosslinking polymerization, *Polym. Int.* 51 (2002) 1141–1150.
- [18] W.E. Hennink, C.F. van Nostrum, Novel crosslinking methods to design hydrogels, *Adv. Drug Deliv. Rev.* 54 (2002) 13–36.
- [19] B. Jeong, S.W. Kim, Y.H. Bae, Thermosensitive sol-gel reversible hydrogels, *Adv. Drug Deliv. Rev.* 54 (2002) 37–51.
- [20] C.D. O'Connell, B. Zhang, C. Onofrillo, S. Duchi, R. Blanchard, A. Quigley, J. Bourke, S. Gambhir, R. Kapsa, C. Di Bella, P. Choong, G.G. Wallace, Tailoring the mechanical properties of gelatin methacryloyl hydrogels through manipulation of the photocrosslinking conditions, *Soft Matter* 14 (2018) 2142–2151.
- [21] J.H.Y. Chung, S. Naficy, Z. Yue, R. Kapsa, A. Quigley, S.E. Moulton, G.G. Wallace, Bio-ink properties and printability for extrusion printing living cells, *Biomater. Sci.* 1 (2013).
- [22] Y. Zhao, Y. Li, S. Mao, W. Sun, R. Yao, The influence of printing parameters on cell survival rate and printability in microextrusion-based 3D cell printing technology, *Biofabrication* 7 (2015) 045002.
- [23] N. Paxton, W. Smolan, T. Bock, F. Melchels, J. Groll, T. Jungst, Proposal to assess printability of bioinks for extrusion-based bioprinting and evaluation of rheological properties governing bioprintability, *Biofabrication* 9 (2017) 044107.
- [24] X.Y. Tian, M.G. Li, N. Cao, J.W. Li, X.B. Chen, Characterization of the flow behavior of alginate/hydroxyapatite mixtures for tissue scaffold fabrication, *Biofabrication* 1 (2009) 045005.
- [25] D. Wu, C. Xu, Predictive modeling of droplet formation processes in inkjet-based bioprinting, *J. Manuf. Sci. Eng.* (2018) 140.
- [26] J. Shi, J. Song, B. Song, W.F. Lu, Multi-objective optimization design through machine learning for drop-on-demand bioprinting, *Engineering* 5 (2019) 586–593.
- [27] S. Greenhill, S. Rana, S. Gupta, P. Vellanki, S. Venkatesh, Bayesian optimization for adaptive experimental design: a review, *IEEE Access* 8 (2020) 13937–13948.
- [28] C. Li, D. Rubin de Celis Leal, S. Rana, S. Gupta, A. Sutti, S. Greenhill, T. Slezak, M. Height, S. Venkatesh, Rapid bayesian optimisation for synthesis of short polymer fiber materials, *Sci. Rep.* 7 (2017) 5683.

- [29] P.I. Frazier, J. Wang, *Information Science for Materials Discovery and Design*, Springer, Cham, 2016.
- [30] N. Srinivas, A. Krause, S. Kakade, M. Seeger, Gaussian process optimization in the bandit setting: no regret and experimental design, in: *Proceedings of the 27th International Conference on International Conference on Machine Learning*, Omnipress, Haifa, Israel, 2010, pp. 1015–1022.
- [31] C.D. O'Connell, C. Di Bella, F. Thompson, C. Augustine, S. Beirne, R. Cornock, C.J. Richards, J. Chung, S. Gambhir, Z. Yue, J. Bourke, B. Zhang, A. Taylor, A. Quigley, R. Kapsa, P. Choong, G.G. Wallace, Development of the Biopen: a handheld device for surgical printing of adipose stem cells at a chondral wound site, *Biofabrication* 8 (2016) 015019.
- [32] C. Rasmussen, C. Williams, *Gaussian Processes for Machine Learning*, Massachusetts Institute of Technology, Cambridge, MA, USA, 2006.
- [33] E. Brochu, V. Cora, N. Freitas, A Tutorial on Bayesian Optimization of Expensive Cost Functions, with Application to Active User Modeling and Hierarchical Reinforcement Learning, *ArXiv*, abs/1012.2599 (2010).
- [34] P. Vellanki, S. Rana, S. Gupta, D. Rubin, A. Sutti, T. Dorin, M. Height, P. Sandars, S. Venkatesh, Process-constrained batch Bayesian optimisation, *Neural Information Processing Systems*, in: *Conference, Neural Information Processing Systems Foundation*, Long Beach, California, 2017, pp. 3415–3424.
- [35] W. Xu, B.Z. Molino, F. Cheng, P.J. Molino, Z. Yue, D. Su, X. Wang, S. Willfor, C. Xu, G.G. Wallace, On low-concentration inks formulated by nanocellulose assisted with Gelatin Methacrylate (GelMA) for 3D printing toward wound healing application, *ACS Appl. Mater. Interface*. 11 (2019) 8838–8848.
- [36] K. Holzl, S. Lin, L. Tytgat, S. Van Vlierberghe, L. Gu, A. Ovsianikov, Bioink properties before, during and after 3D bioprinting, *Biofabrication* 8 (2016) 032002.